# Polarization studies in $t\bar{t}$ semileptonic events (part of T7 CSC note)

**C. Feng, C. Zhu**

School of physics and micro-electronics, Shandong University, Jinan - China

**F. Hubaut, E. Monnier, P. Pralavorio**

Centre de Physique des Particules de Marseille, CNRS/IN2P3 - Univ. Méditerranée, Marseille - France

# Contents

# 1 Introduction

The measurements of $W$ boson and top quark polarization in $t\bar{t}$ events provide powerful tests of top production and decay mechanisms and are sensitive probes to new physics. $W$ (top) spin information can be inferred from angular distributions of the daughter particles in the $W$ (top) rest frame:

- The three $W$ helicity state probabilities, $F_0$ (longitudinal), $F_L$ (left-handed) and $F_R$ (right-handed), can be extracted from the $\Psi$ angular distribution [1] :

$$\frac{1}{N}\frac{dN}{d\cos\Psi} = \frac{3}{2}\left[F_0\left(\frac{\sin\Psi}{\sqrt{2}}\right)^2 + F_L\left(\frac{1-\cos\Psi}{2}\right)^2 + F_R\left(\frac{1+\cos\Psi}{2}\right)^2\right] \quad (1)$$

  where $\Psi$ is the angle between the charged lepton direction in the $W$ rest frame and the $W$ direction in the top quark rest frame.

- The production asymmetry in $t\bar{t}$ event is :

$$A = \frac{\sigma(t_\uparrow\bar{t}_\uparrow) + \sigma(t_\downarrow\bar{t}_\downarrow) - \sigma(t_\uparrow\bar{t}_\downarrow) - \sigma(t_\downarrow\bar{t}_\uparrow)}{\sigma(t_\uparrow\bar{t}_\uparrow) + \sigma(t_\downarrow\bar{t}_\downarrow) + \sigma(t_\uparrow\bar{t}_\downarrow) + \sigma(t_\downarrow\bar{t}_\uparrow)}, \quad (2)$$

  where $\sigma(t_{\uparrow/\downarrow}\bar{t}_{\uparrow/\downarrow})$ denotes the production cross section of a top quark pair with spins up or down with respect to a quantization axis. It can be extracted from the $\theta_1$ and $\theta_2$ angular distribution [2] :

$$\frac{1}{N}\frac{d^2N}{d\cos\theta_1 d\cos\theta_2} = \frac{1}{4}(1 - A|\alpha_1\alpha_2|\cos\theta_1\cos\theta_2) \quad (3)$$

  where $\theta_1$ ($\theta_2$) is the angle between the direction of the $t$ ($\bar{t}$) daughter in the $t$ ($\bar{t}$) rest frame and the $t$ ($\bar{t}$) direction in the $t\bar{t}$ center of mass system. $\alpha_i$ is the spin analyzing power of particle $i$, i.e. the degree to which its direction is correlated to the spin of the parent top quark, ranging between -1 and 1.

- The production asymmetry $A_D$, which can also be cast into the form shown in Equation (2), is extracted from the $\Phi$ angular distribution [2] :

$$\frac{1}{N}\frac{dN}{d\cos\Phi} = \frac{1}{2}(1 - A_D|\alpha_1\alpha_2|\cos\Phi) \quad (4)$$

  where $\Phi$ is the angle between the direction of flight of the two spin analyzers, defined in the $t$ and $\bar{t}$ rest frames respectively.

The Standard Model (SM) predictions for $W$ boson polarization ($F_0$, $F_L$, $F_R$) at next-to-leading order and $t\bar{t}$ spin correlation ($A$, $A_D$) at leading order are given in Table 1. The ATLAS sensitivity to these observables has been evaluated with a fast simulation [3] and a perfect detector simulation [4]. A precision of 1 to 5% should be achievable with 10 fb$^{-1}$ of data dominated by systematic uncertainties especially coming from the $b$-jet energy scale. These measurements require a complete reconstruction of the $t\bar{t}$ system and a reliable Monte-Carlo description to correct for the biases induced by reconstruction and cuts. The purpose

| $F_0$ | $F_L$ | $F_R$ | A* | $A_D$* |
|---|---|---|---|---|
| 0.695 | 0.304 | 0.001 | 0.422 | -0.290 |

Table 1: *SM values of W boson polarization ($F_0$, $F_L$, $F_R$) at next-to-leading oder and $t\bar{t}$ spin correlation (A, $A_D$) at leading order for a top mass of 175 GeV. * $M_{t\bar{t}} < 550$ GeV is applied for A and $A_D$ [6].*

of this note is to assess the robustness of the analysis with a realistic detector simulation [5] including triggering. Only semileptonic channel ($t\bar{t} \to WWb\bar{b} \to l\nu j_1 j_2 b\bar{b}$ with $l = e, \mu$) is used as signal. In this case the most powerful spin analyzers of the top are the charged lepton ($\alpha_1 = 1$) and the least energetic non-b jet in the top rest frame ($\alpha_{lej} = 0.51$) [6].

# 2 Event simulation

With a next-to-leading order (NLO) cross-section around 850 pb [7], 3.8 millions of $t\bar{t}$ semileptonic events will be produced for an integrated luminosity of 10 fb$^{-1}$, corresponding to one LHC year at low luminosity ($10^{33}$cm$^{-2}$s$^{-1}$). Among those, 2.5 millions are signal events ($t\bar{t} \to WbW\bar{b} \to l\nu bq_1q_2\bar{b}$ with $l = e, \mu$) while 1.3 million events with $l = \tau$ are considered as background. Non-$t\bar{t}$ background is dominated by $W + n$ partons and single top productions [3].

## 2.1 Event generation

The samples used in this study are part of the ATLAS CSC (Computing System Commissioning) data. Generation of $t\bar{t}$ events (CSC data set 5200) is done using next-to-leading-order (NLO) generator MCatNLO 3.1, which doesn't include standard model $t\bar{t}$ spin correlation[8]. A fixed top mass of 175 GeV is assumed. Partons are fragmented and hadronized using HERWIG 6.510 [9]. Background events coming from $W + n$ partons are generated with AlpGen [10], while the single tops are generated with AcerMC. They all contain one $W$ decaying leptonically ($W \to l\nu$). TAUOLA and PHOTOS [11] are used to process the $\tau$-decay and radiative corrections. Initial, final state radiations and multiple interactions are simulated in agreement with CDF data extrapolated to LHC [12]. No pile-up events are added. The complete list of data samples used throughout this note is given in Table 2.

Besides, for the study of spin correlation of $t\bar{t}$, a sample (CSC data set 5205) generated with AcerMC at leading order level, partons fragmented and hadronized using Pythia 6.403 is used. TAUOLA and PHOTOS are used to process the $\tau$-decay and radiative corrections.

## 2.2 Detector modeling

Once those events are produced, they are passed through a complete GEANT4 detector simulation with version 12.0.31 of ATLAS software. The used ATLAS layout version CSC-01-02-00 is based on a perfect detector, with misaligned layout of LAr and Muons system, distorted materials in LAr and inner detector, magnetic field with initial displacement included. The signals of each sub-detector are digitized and the whole event is reconstructed with ATLAS software

| Event type | Generator | Sample reference | Integrated luminosity ($pb^{-1}$) | Number of events |
|---|---|---|---|---|
| **Signal** | | | | |
| $t\bar{t} \to l\nu bq_1q_2\bar{b}$ $(l = e, \mu, \tau)$ | MCatNLO | 5200 | 730 | 270 500 |
| $t\bar{t} \to l\nu bq_1q_2\bar{b}$ $(l = e, \mu, \tau)$ | AcerMC | 5205 | 220 | 81 000 |
| **Background** | | | | |
| $W(\to e\nu)$+2p | AlpGen | 8240 | 103 | 22 000 * |
| $W(\to e\nu)$+3p | AlpGen | 8241 | 89 | 11 000 |
| $W(\to e\nu)$+4p | AlpGen | 8242 | 112 | 6 000 |
| $W(\to e\nu)$+5p | AlpGen | 8243 | 224 | 5 000 |
| $W(\to \mu\nu)$+2p | AlpGen | 8244 | 92 | 1 500 |
| $W(\to \mu\nu)$+3p | AlpGen | 8245 | 143 | 9 300 |
| $W(\to \mu\nu)$+4p | AlpGen | 8246 | 82 | 3 200 |
| $W(\to \mu\nu)$+5p | AlpGen | 8247 | 224 | 4 500 |
| $W(\to \tau\nu)$+2p | AlpGen | 8248 | 197 | 17 300 |
| $W(\to \tau\nu)$+3p | AlpGen | 8249 | 149 | 13 000 |
| $W(\to \tau\nu)$+4p | AlpGen | 8250 | 109 | 5 000 |
| Single top (Wt) | AcerMC | 5500 | 990 | 25 300 |
| Single top (Wg) | AcerMC | 5502 | 185 | 15 000 |

Table 2: *List of CSC data samples used in this study. * All w+np events are filtered before detector simulation.*

version 12.0.6 including triggering simulation. Object style reconstructed outputs (AOD) are used in the analysis. An extensive comparison with the perfect detector simulation (so-called "Rome" samples) results [4] is proposed throughout the analysis.

# 3 Event selection

Semileptonic signal events are characterized by one (and only one) isolated lepton, at least 4 jets, of which at least 2 are b-jets, and missing transverse energy.

## 3.1 Leptons

### 3.1.1 Electrons

Electrons are identified and reconstructed with the egamma high $p_T$ algorithm (no cut on the TRT threshold hits). An isolation cut is applied on the calorimeter activity around the electron cluster: $E_T$ (EM+HAD in $\Delta R = 0.2$)<6 GeV. Selecting events containing only one isolated electron with $p_T$ >20 GeV and $|\eta| < 2.5$ yields an efficiency of 51%. The lower selecting efficiency comparing with "Rome" result (63%) is due to the lower electron reconstruction efficiency.

The averaged reconstruction efficiency for true electrons ($p_T > 20$GeV and $|\eta| < 2.5$) in $t\bar{t}$ events is 69.8%, lower than "Rome" result (85.6%), due to the significantly increased ID material (especially in the endcap region). The upper part of Figure 1 shows the reconstruction efficiency evolution as a function of $\eta$ (left) and $p_T$ (right), with "Rome" reuslt superimposed. The degradation of reconstruction efficiency, especially in the endcap region is visible. Comparing the $p_T$ of reconstructed electron and its corresponding truth one ($\Delta R < 0.1$), the resolution is obtained. A -2.7% shift of the peak is obtained. This is caused by a problem in CSC simulation, which set the range cutoff in LAr volumes to GEANT4 default value of 1mm rather than ATLAS value of 30$\mu$m. This affects the response to the electron energy deposition. In the analysis, the recorded energy in AOD files in the EM layer deposited by electron is corrected according to its $\eta$ manually, while with energy in presampler unchanged.

### 3.1.2 Muons

Muons are identified and reconstructed in the muon spectrometer with the Moore high $p_T$ algorithm. Cuts ($\chi^2$/NDF< 20) on performance of track extrapolation to ID and isolation (ET (EM in $\Delta R = 0.2$)< 6GeV) are used to purify muon selections. Selecting events with only one isolated muon with $p_T > 20$GeV and $|\eta| < 2.5$ yields an efficiency of 67.7% (higher than "Rome" result 60%), due to the higher muon reconstruction efficiency. The purity is very high(99.3%).

The averaged reconstruction efficiency for the true muons ($p_T$> 20GeV and $|\eta| < 2.5$) in $t\bar{t}$ events is 91.4%, higher than the "Rome" result (83%), after the reparation of the recognition algorithm in the endcap region. It is illustrated in the lower part of Figure 1 as a function of $\eta$ (left) and $p_T$(right). A uniformity of reconstruction efficiency as function of $\eta$ is visible.

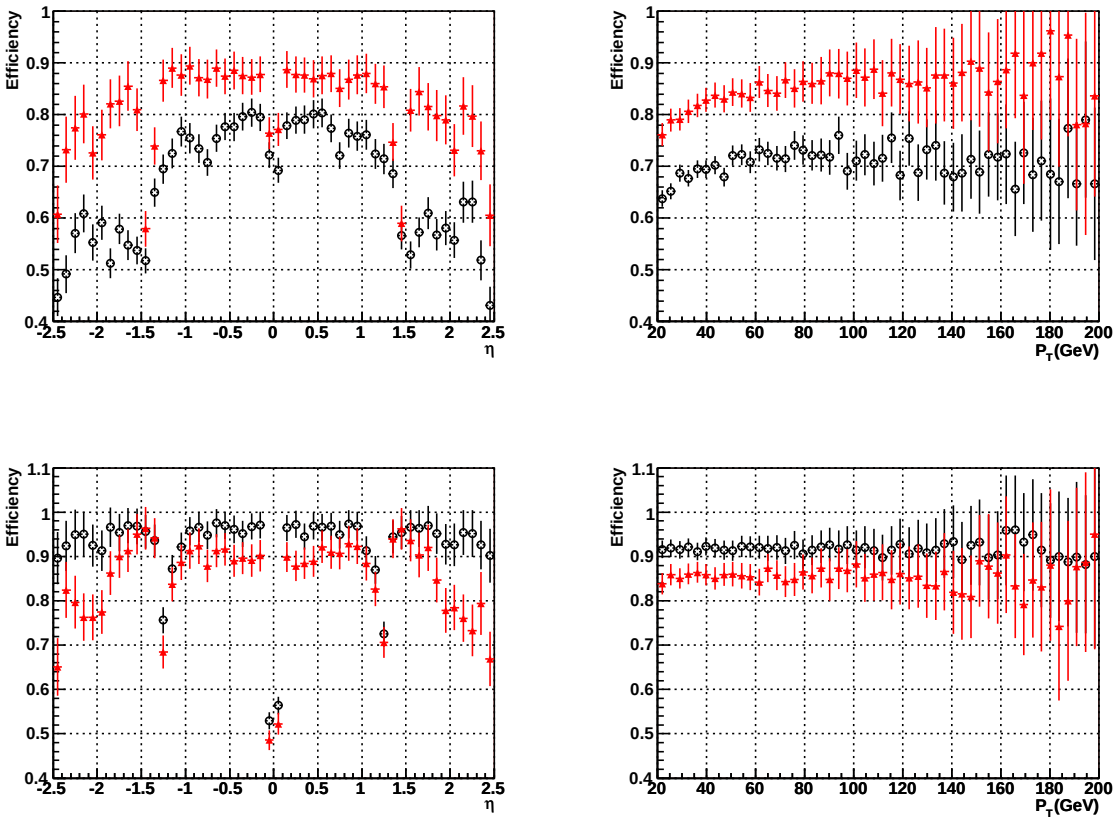


Figure 1: *Reconstruction efficiencies of electrons (up) and muons (down) (true* $p_T$ *>20 GeV and* $|\eta| < 2.5$*) as a function of* $\eta$ *and* $p_T$*. "Rome" results are superimposed(solid triangle). No TRT cut on High Threshold hits is included for electrons.*

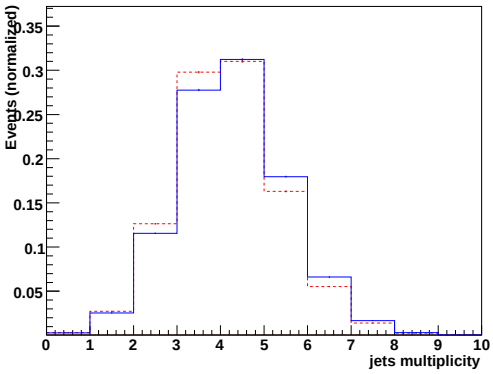


Figure 2: *jet multiplicity in one event. dotted line for "Rome" results and solid line for CSC results(MCatNLO)*

## 3.2 Jets

Jets are reconstructed in the calorimeters with a cone algorithm of size $\Delta$R=0.4. Corrections on jet energy from leptons and energy calibration to truth quark are performed with method used in "Rome" analysis [4]. Events are kept if more than 4 jets with $p_T > 30$GeV and $|\eta| < 2.5$ are found. The selection efficiency is 58% ("Rome" 55%), due to a little bit higher jet multiplicity (Figure 2).

In order to compare with the "Rome" analysis, a compatible b-tagging efficiency is preferred. In CSC production, the weight(SV1+IP3D) for jets shifts up (Figure 3 left). A compatible b-tagging efficiency indicates a higher cut on weight(SV1+IP3D) than "Rome" analysis. We use weight(SV1+IP3D)$>$ 6.5 to tag b jet, which corresponds to a b-tagging efficiency 60.8%, with a rejection factors of $R_{uds}$=131 and $R_c$=6.9, as illustrated in Figure 3 (right). The compatible b-tagging efficiency with lower light jet rejection than "Rome" indicates a slightly degraded b-tagging performance.

Within all the selected jets in one event, at least two are required to be tagged as b jet. With this requirement, 32% of events is reserved from the events with more than 4 jets.

## 3.3 Missing transverse momentum

The missing transverse energy is calculated by retrieving the calorimeter energy in topological clusters, and compensating for energy losses upstream (in the cryostat) and carried by muons. The cut of $p_T^{miss} > 20$ GeV yields an efficiency of 92%, in good agreement with "Rome" samples (91%).

## 3.4 Kinematic selection efficiency

All kinematic cuts are summarized in Table 3. Their overall efficiency on signal events is 9.5%, in good agreement with "Rome" results, under compensation between improvement of muons

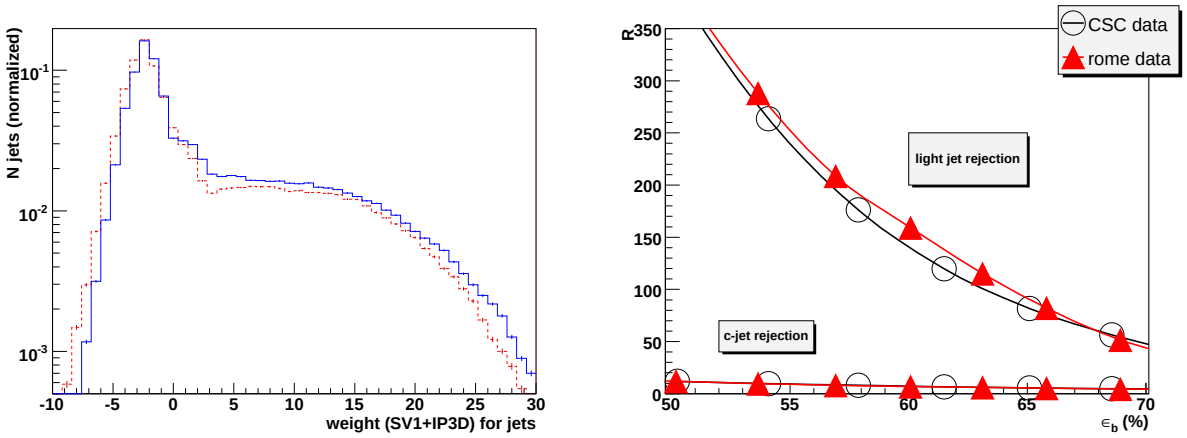


Figure 3: *left: b-tagging weight(SV1+IP3D) for all jets for CSC data (solid line) and "Rome" data (dotted line) . right: Light jets (up) and c-jets (down) rejection as a function of the b-tagging efficiency, for CSC data (open cycle) and "Rome" data (triangle).*

and degradation of electrons. A selection efficiency of 10.0% is obtained for the data set 5205 generated with AcerMC.

| Variables | Cuts | Efficiency (%) | |
|---|---|---|---|
| | | full sim (Rome) | full sim (CSC) |
| =1 isolated lepton | $p_T > 20$ GeV, $\|\eta\| < 2.5$ | 62 | 59 |
| $\geq 4$ jets | $p_T > 30$ GeV, $\|\eta\| < 2.5$ | 55 | 58 |
| *b*-tagging | $\geq 2$ b-jets | 32 | 32 |
| Missing energy ($\nu$) | $p_T^{miss} > 20$ GeV | 90 | 92 |
| Global efficiency | | 9.5 | 9.5 |

Table 3: *Selection cuts and corresponding efficiencies on semileptonic $t\bar{t}$ MCatNLO events in "Rome" data and CSC data.*

# 4 $W$ polarization and $t\bar{t}$ spin correlation measurements

After kinematic cuts are applied, the event is fully reconstructed. Angles $\Psi$, $\theta_1$, $\theta_2$ and $\Phi$ are computed and polarization parameters are extracted.

## 4.1 $W$ and top reconstruction

The light jet pair with $M_{jj}$ closest to the known $W$ mass, $M_W$ [15], is selected to reconstruct the hadronic decayed $W$. The event is kept if the difference between this invariant mass and $M_W$ is less than 20 GeV. The hadronic decayed $W$ and the $b$-jet, whose invariant mass $M_{jjb}$ are closest to $M_t$ [15], are then used to reconstruct the top quark. The $b$-jet, which is closest to the lepton in $\Delta R$ among the remaining $b$-jets, is reserved for reconstructing the other top quark with the leptonic decayed $W$. To reconstruct the leptonic decayed $W$, the neutrino $p_T$ is assumed to be the missing transverse momentum. Its longitudinal component $p_z$ is determined by constraining $M_{l\nu}$ to $M_W$ [4]. When two solutions are found, the one with $M_{l\nu b}$ closest to M$t$ is kept. No solution is found for one third of the events, due to $p_T^{miss}$ resolution. A procedure to recover these events was applied [3].

Quality cuts are applied on these reconstructed masses ($|M_{hadt} - M_t| < 35$GeV and $|M_{lept} - M_t| < 35$GeV) to reject badly reconstructed events. At this stage, 2.9% of the signal events are kept (2.8% for AcerMC events), corresponding to 72500 signal events for 10 fb$^{-1}$ of data (Table 4), with a good agreement with "Rome" results (2.7%). After selection, the background is dominated by $t\bar{t} \to \tau + X$ events. The polarization study in the following sections will take only the $t\bar{t} \to \tau + X$ events as background. The numbers of remaining signal and background events for 10 fb$^{-1}$ of data are listed in Table 4.

| | Events for 10 fb$^{-1}$($\times 10^6$) | Selected events full sim Rome | Selected events full sim CSC |
|---|---|---|---|
| **Signal** ($t\bar{t}$ semileptonic) | 2.5 | 70000 | 72500 |
| $t\bar{t} \to \tau + X$ | 1.3 | 7500 | 7400 |
| $W(\to l\nu)$+np | 8 * | 900 ** | <2300 |
| single top 5500 | 0.25 $^{\Delta}$ | 550 | 900 |
| single top 5502 | 0.8 | 250 | 550 |

Table 4: *The number of signal and background events before (left) and after (right) selection with 10 fb$^{-1}$. *: Filtered before detector simulation. **: For "Rome" w+4jets events. $\Delta$: All single top data including $W \to \tau\nu$ mode*

## 4.2 $W$ polarization

After reconstruction of the whole event, the $\Psi$ angle is computed using $W$ and top rest frames on the leptonic side. The resolution on this angle is shown on Figure 4, where a perfect agreement

between CSC and "Rome" data is achieved. To correct the bias on distribution induced by reconstruction and cut effects, the same correction function used in "Rome" analysis, is taken. Figure 5 shows the correction function on left and the reconstructed cos$\Psi$ distribution after correction on right. It is fitted with Eq. (1) and the constraint $F_0 + F_L + F_R = 1$. The fit results, shown in Table 5, are consistent with "Rome" results.

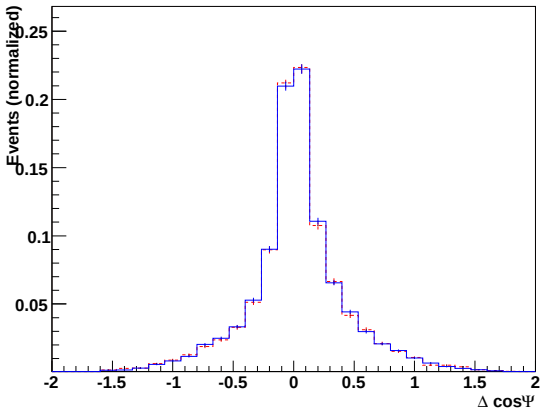


Figure 4: *the resolution of reconstructed cos$\Psi$ for CSC data (solid line), with "Rome" result superimposed (dotted line).*

| | $F_L$ | $F_0$ | $F_R$ | $A$ | $A_D$ |
|---|---|---|---|---|---|
| Full sim CSC. | 0.29 $\pm$ 0.02 | 0.71$\pm$0.03 | 0.00$\pm$ 0.03 | 0.65 $\pm$ 0.17 | -0.36 $\pm$ 0.10 |
| Full sim Rome. | 0.29 $\pm$ 0.02 | 0.71$\pm$0.04 | 0.00$\pm$ 0.02 | 0.67 $\pm$ 0.10 | -0.33 $\pm$ 0.06 |

Table 5: *W polarization and top spin correlation parameters extracted from the "Rome" and CSC samples. Errors indicated are only statistical.*

## 4.3 $t\bar{t}$ spin correlation

To evaluate the measurement of $t\bar{t}$ spin correlation, the data set 5205 generated with AcerMC is used. the angles $\theta_1$, $\theta_2$ and $\Phi$ are computed using lepton, least energy jet in the rest frame of $t$ quarks and $t$ quarks in the $t\bar{t}$ rest frame . The resolutions of the three angles are compatible with the "Rome" results. To correct the bias of distribution induced by reconstruction and selection, correction functions computed with atlas fast simulation data are used here. Figure 6 shows the reconstructed $\cos\theta_1 * \cos\theta_2$ distribution after correction, the mean corresponding to the asymmetry parameter $A$, after divided by analyzer power 0.51. The same evaluation is done to $\cos\Phi$, as in Figure 7, whose mean corresponds to asymmetry parameter $A_d$, after divided by analyzer power 0.51. The result of $A$ and $A_d$ are shown in Table 5, which are consistent with "Rome" results.

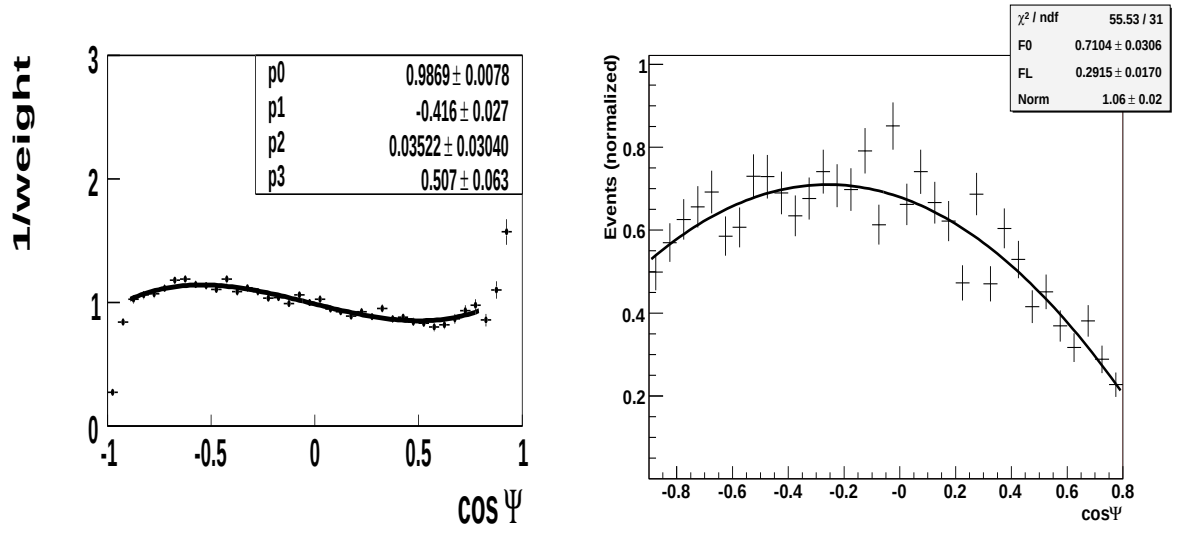


Figure 5: *Left: ratio between the reconstructed and parton level* $\cos\Psi$ *distributions for the fast simulation. The third order polynomial fitting function is the correction function. Right: Normalized reconstructed and corrected* $\cos\Psi$ *distribution. The line corresponds to the fit with Eq. (1).*

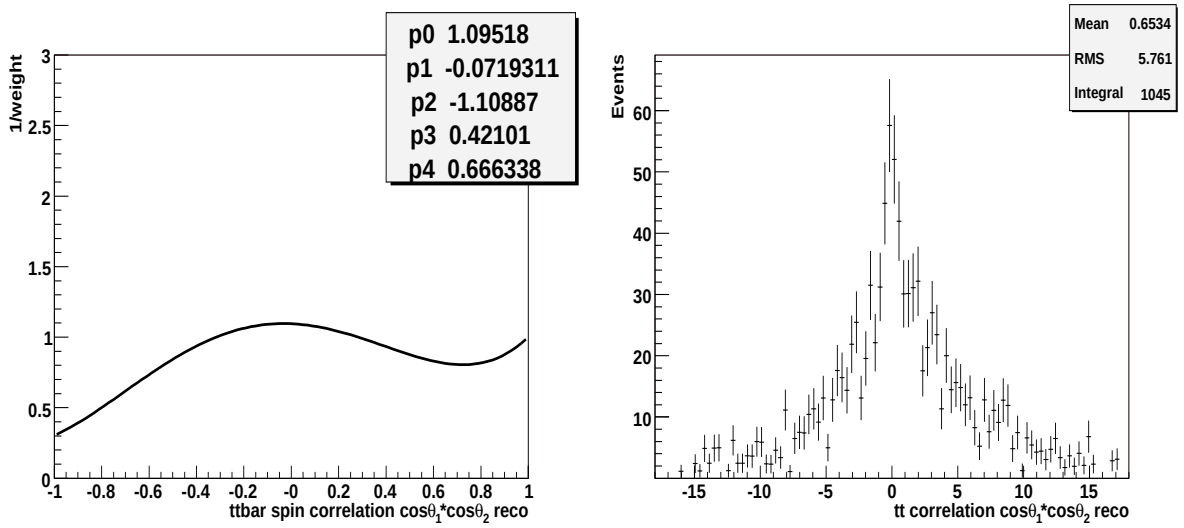


Figure 6: *Left: ratio of* $\cos\theta_1 * \cos\theta_2$ *distributions between the reconstructed and parton level with fast simulation, used to correct the reconstructed* $\cos\theta_1 * \cos\theta_2$ *distribution. Right: Reconstructed and corrected* $\cos\theta_1 * \cos\theta_2$ *distribution. The mean corresponds to the asymmetry parameter A, after divided by analyzer power 0.51*

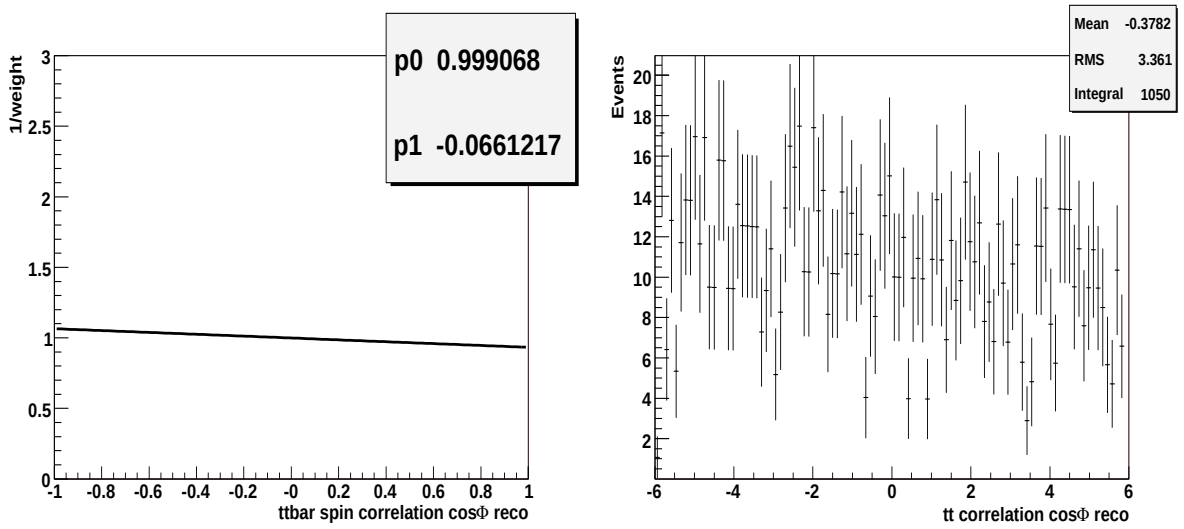


Figure 7: *Left: ratio of* $\cos\Phi$ *distributions between the reconstructed and parton level with fast simulation, used to correct the reconstructed* $\cos\Phi$ *distribution. Right: reconstructed and corrected* $\cos\Phi$ *distribution. The mean corresponds to the asymmetry parameter* $A_d$*, after divided by analyzer power 0.51*

# 5 Impact of the trigger on the analysis

Due to imperfect selection efficiency of the online level 1 trigger and offline high level trigger, some good events may lose and bias is introduced. In this section, this effects are studied. The semileptonic decayed $t\bar{t}$ events are characterized by a single isolated lepton, which can be used to trigger the majority of the events. So we concentrate only on the lepton trigger.

## 5.1 Level one trigger

The level 1 trigger is an online trigger, making fast decision to accept event which passes predefined criteria. Several trigger items on lepton have been defined in ATLAS. The ones match our needs are "$L1\_EM25I$" for triggering isolated electron and "$L1\_MU20||L1\_MU40$" for triggering muon, according to our selection criterias. Their aims are to trigger lepton with $p_T$ more than 25 GeV (isolated electron) or 20 GeV (muon) with a high efficiency (98%).

Taking the events which have one electron or one muon selected by the method described in section 3, we then look at the level 1 trigger decision on these events. The trigger efficiency is defined as percentage of analysis selected leptons which are triggered. The level 1 trigger efficiencies as function of $\eta$, $p_T$ and $\phi$ are shown in Figure 8 with thin solid line. Uniformed efficiencies can be seen, in despite of the affection on muon from ATLAS feet support structure.

With the level 1 trigger on lepton, 5% of good $t\bar{t}$ events decayed to electron and 13% decayed to muon are lost. The value is 9% for combining both.

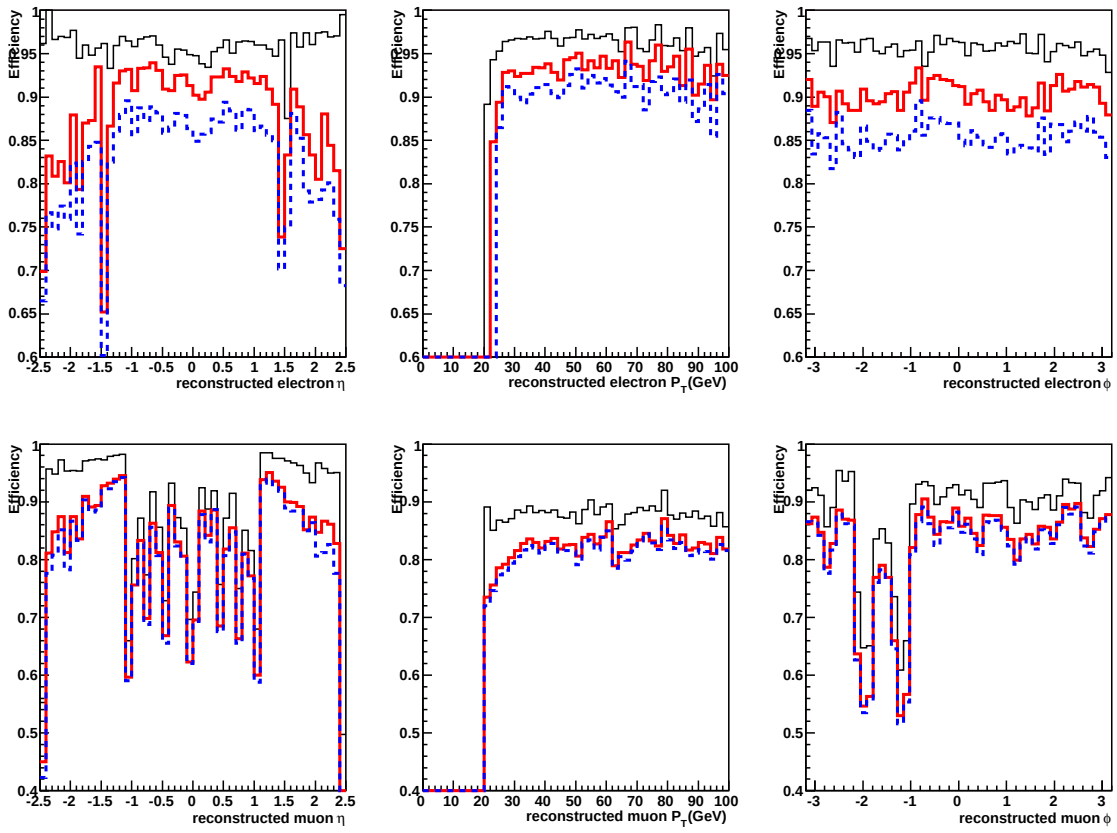


Figure 8: *Isolated electron ($p_T > 25GeV$) trigger efficiency (up) and muon ($p_T > 20GeV$) trigger efficiency (down) on analysis selected good ones as function of* η, $p_T$ *and* ϕ. *thin solid line: level 1 trigger efficiency; thick solid line: level 2 trigger efficiency; dashed line: event filter efficiency.*

### 5.2 High level trigger

The high level trigger consists of level 2 trigger and event filter, operating on events triggered by level 1. Following the trigger mechanism used above in level 1, the trigger "$L2\_e25i$" and "$L2\_mu20i$", "$EF\_e25i$" and "$EF\_mu20i$" are the corresponding refining trigger, in level 2 trigger and event filter. The refining process rejects good events further, as shown Figure 8, thick solid line and dashed line. It's clear that lepton in ATLAS endcap region are less triggered by high level trigger. The bias could be introduced by the facts that electron with $p_T$ less than 25 GeV are almost all rejected and more muon with $p_T$ close to 20GeV are rejected.

With three level triggers on lepton, finally 17% of good $t\bar{t}$ semileptonic decayed events are lost. With the affection of each level of trigger, the measurements of $W$ polarization and $t\bar{t}$ spin correlation are slightly biased, see table 6. This trigger induced bias is not neglectable, and should be included into correction function.

| | $F_L$ | $F_0$ | $F_R$ | $A$ | $A_D$ |
|---|---|---|---|---|---|
| level 1 trigger | 0.29 $\pm$ 0.02 | 0.70$\pm$0.04 | 0.01$\pm$ 0.03 | 0.61 $\pm$ 0.18 | -0.35 $\pm$ 0.11 |
| level 2 trigger | 0.28 $\pm$ 0.03 | 0.71$\pm$0.04 | 0.02$\pm$ 0.03 | 0.56 $\pm$ 0.19 | -0.38 $\pm$ 0.11 |
| event filter | 0.26 $\pm$ 0.03 | 0.73$\pm$0.04 | 0.01$\pm$ 0.03 | 0.59 $\pm$ 0.19 | -0.36 $\pm$ 0.11 |

Table 6: *$W$ and top spin correlation parameters with affection of each level of triggers. Errors indicated are only statistical.*

# 6 Conclusions

A complete study of the $W$ polarization and $t\bar{t}$ spin correlation with a realistic detector simulation has been performed in the semileptonic $t\bar{t}$ channel. A consistent selection efficiency 2.9%, corresponding to 72500 signal events with 10 fb$^{-1}$, is obtained. Reconstructed and corrected angular distributions in $W$ and top rest frames are used to extract polarization measurements. Results are in a good agreement with "Rome" values assessing the robustness of the method.

# References


[1] G.L. Kane, G.A. Ladinsky and C.-P. Yuan, *Using the top quark for testing standard-model polarization and CP predictions*, Phys. Rev. **D 45** (1992) 124.

[2] W. Bernreuther *et al.*, *Top quark pair production and decay at hadron colliders*, Nucl. Phys. **B 690** (2004) 81, hep-ph/0403035.

[3] F. Hubaut *et al.*, *ATLAS sensitivity to top quark and $W$ boson polarization in $t\bar{t}$ event*, Eur. Phys. J. **C 44 S2** (2005) 13, hep-ex/0508061.

[4] F. Hubaut *et al.*,*Polarization studies in $t\bar{t}$ semileptonic events with ATLAS full simulation*, ATL-PHYS-PUB-2006-022.

[5] A. Ahmad *et al.*,*Inner detector as-built detector description validation for CSC*, ATL-COM-INDET-2007-012.

[6] F. Hubaut, E. Monnier and P. Pralavorio, *ATLAS sensitivity to $t\bar{t}$ spin correlation in the semileptonic channel*, ATL-PHYS-PUB-2005-001.

[7] R. Bonciani *et al.*, *NLL resummation of the heavy quark hadroproduction cross-section*, Nucl. Phys. **B 529** (1998) 424, hep-ph/9801375.

[8] S. Frixione and B. Webber, *The MCatNLO 3.1 Event Generator*, hep-ph/0506182.

[9] G. Corcella *et al.*, *HERWIG 6.5: an event generator for hadron emission reactions with interfering gluons (including supersymmetric processes)*, JHEP01 (2001) 010, hep-ph/0011363.

[10] M. L. Mangano *et al.*, *Alpgen, a generator for hard multiparton processes in hadronic collisions*, JHEP07 (2003) 001, hep-ph/0206293.

[11] P. Golonka *et al.*, *The tauola-photos-F environment for the TAUOLA and PHOTOS packages, release II*, CERN-TH/2003-287, hep-ph/0312240.

[12] A. Moraes, C. Buttar and I. Dawson, *Prediction for Minimum Bias and the Underlying Event at LHC Energies*, ATL-PHYS-PUB-2005-007.

[13] S. Agostinelli *et al.*, *GEANT4: A Simulation toolkit*, Nucl. Instrum. Methods **A506** (2003) 250.

[14] E. Richter-Was, D. Froidevaux and L. Poggioli, *ATLFAST 2.0 a fast simulation package for ATLAS*, ATL-PHYS-98-131.

[15] S. Eidelman *et al.*, *Review of particle Physics. Particle Data Group*, Phys. Lett. **B 592** (2004), 1.

[16] F. Hubaut *et al.*, *Comparison between full and fast simulations in top physics*, ATL-PHYS-PUB-2006-017.